Ceramics International 43 (2017) 2022–2026

Contents lists available at ScienceDirect

Ceramics International

journal homepage: www.elsevier.com/locate/ceramint

# Antiferromagnetism and heat capacity of $NaCo_{2-x}Cu_xO_4$ ceramics

Sanja Pršić[a,*], Slavica M. Savić[a,b], Zorica Branković[a], Zvonko Jagličić[c,d], Stanislav Vrtnik[e], Goran Branković[a]

[a] Institute for Multidisciplinary Research, University of Belgrade, Kneza Višeslava 1a, 11030 Belgrade, Serbia
[b] Biosense Institute-Institute for Research and Development of Information Technology in Biosystems, Dr Zorana Đinđića 1, 21000 Novi Sad, Serbia
[c] Faculty of Civil and Geodetic Engineering, University of Ljubljana, Jamova Cesta 2, 1000 Ljubljana, Slovenia
[d] Institute of Mathematics, Physics and Mechanics, Jadranska 19, 1000 Ljubljana, Slovenia
[e] Jožef Stefan Institute, Condensed Matter Physics, Jamova cesta 39, 1000 Ljubljana, Slovenia

ARTICLE INFO

*Keywords:*
Powders: chemical preparation
Solid state reaction
Sintering
Magnetic properties
Heat capacity

ABSTRACT

Polycrystalline samples of $NaCo_{2-x}Cu_xO_4$ (x=0, 0.01, 0.03 and 0.05) were synthesized in two different ways: 1) by a mechanochemically assisted solid-state reaction method (MASSR) and 2) by a citric acid complex method (CAC). In this work we examined the influence of these synthesis routes and small Cu concentrations on magnetic properties and the heat capacity of sintered samples. The magnetic susceptibility ($\chi$) of all samples followed the Curie-Weiss law in the temperature range between 50 K and 300 K, while a negative Weiss constant ($\theta$) implied an antiferromagnetic interaction. According to the magnetic susceptibility data, a peak around 30 K indicating the presence of $Co_3O_4$ as a secondary phase appeared for all MASSR samples and CAC samples with Cu content above 1%. The effective magnetic moment ($\mu_{eff}$) of CAC samples was lower than the theoretical, spin only value obtained for the $Co^{4+}$ ion in the low spin state indicating the presence of low spin $Co^{3+}$(S =0). These values were also lower compared to the values obtained for MASSR samples. The highest $\mu_{eff}$ of 1.75 $\mu_B$/atom Co was obtained for the undoped MASSR sample. The heat capacity of CAC samples at 2 K decreased with Cu concentration due to lowering of the electronic specific heat coefficient ($\gamma$). The highest $\gamma$ of 63.9 mJ/molK$^2$ was obtained for the undoped CAC sample. This reduction in $\gamma$ values was the result of the decrease of the density of state and/or mass enhancement factor.

## 1. Introduction

In the past few decades, there has been a growing interest in alternative energy sources and new methods for energy conversion. Thermoelectric materials belong to the group of materials that directly convert waste heat into electric energy. Among them, layered oxides attract great attention because of their interesting structural, physical and chemical properties, such as $NaCo_2O_4$ (NCO), which exhibits good thermoelectric properties [1–3]. Increase of the Seebeck coefficient ($S$), simultaneously with the decrease of thermal conductivity ($\kappa$) and electrical resistivity ($\rho$) are the main requests for high thermoelectric performance [4]. High $S$ (also called thermopower) as a consequence of a strong electron correlation and low $\rho$ make $NaCo_2O_4$ a promising material for potential use in thermoelectric devices [5,6].

$NaCo_2O_4$ belongs to compounds with a bronze-type crystal structure of the $A_xBO_2$ ($0.5 \le x \le 1$) general formula [7]. This layered oxide consists of Na and $CoO_2$ layers alternately stacked along the c-direction. The stoichiometry of Na in this compound is variable, and depending on the sodium content, there are three types of crystal structure: P3: β–$Na_xCo_2O_4$ ($1.1 \le x \le 1.2$), P2: γ–$Na_xCo_2O_4$ ($1.0 \le x \le 1.4$), O3: α–$Na_xCo_2O_4$ ($1.8 \le x \le 2.0$), whereby the P2 structure possesses the highest thermopower [8]. As arrangement of sodium ions in the crystal lattice depends on the temperature and Na content [9], diversity of $Na_xCo_2O_4$ properties comes from the different sodium content, accordingly [10].

In general, cobalt oxides are systems with a strong electron correlation, where 3d orbitals have a specific degeneration, due to the spin and orbital degrees of freedom. Two competitive processes are responsible for degeneration of electronic states of $Co^{3+}$ and $Co^{4+}$ ions: crystalline field and Hund's rule coupling [11]. Interactions between 3d electrons largely affect the transport properties of all cobaltites and they are expected to affect magnetic properties of these materials, as well [12]. In the octahedral crystal field, as is the case in the $CoO_2$ layer, the 3d orbitals split into two $e_g$ and three $t_{2g}$ orbitals, which in the rhombohedral crystal field further split into $e'_g$ and $a_{1g}$ orbitals [13–15]. Hybridization between these orbitals causes the formation of two

* Corresponding author.
*E-mail addresses:* sanjaprsic@imsi.rs, sanjaprsic@gmail.com (S. Pršić), slavicas@imsi.bg.ac.rs (S.M. Savić), zorica.brankovic@imsi.bg.ac.rs (Z. Branković), zvonko.jaglicic@imfm.si (Z. Jagličić), stane.vrtnik@ijs.si (S. Vrtnik), goran.brankovic@imsi.bg.ac.rs (G. Branković).

http://dx.doi.org/10.1016/j.ceramint.2016.10.170
Received 1 September 2016; Received in revised form 17 October 2016; Accepted 26 October 2016
Available online 28 October 2016

Fermi surfaces [13]. Basically, the magnetic susceptibility and the electronic specific heat coefficient are proportional to the density of states, which is determined by a large Fermi surface [13].

It is assumed that stoichiometric $NaCo_2O_4$ consists of equal amounts of $Co^{4+}$ and $Co^{3+}$ ions [16]. These ions can occupy one of the following spin states: low spin state, with electronic configurations $t_{2g}^5$ ($t_{2g}^6$); intermediate, $t_{2g}^4e_g^1$ ($t_{2g}^5e_g^1$); or high spin state $t_{2g}^3e_g^2$ ($t_{2g}^4e_g^2$). The occupancy of spin states is dependent on the electron pairing energy and level splitting [15]. The low spin $Co^{4+}$ ions are magnetic (with a spin quantum number of S=1/2) and the $Co^{3+}$ ions are non magnetic (S=0) [11,16]. It is assumed that both $Co^{4+}$ and $Co^{3+}$ ions are in the low spin state in sodium cobaltite, and that is one of the reasons for high thermopower [11,14]. Mixed valence of Co ions in the low spin state is responsible for metallic conductivity of sodium cobaltite [17].

The magnetic properties of $Na_xCoO_2$ depend on the sodium content (x). For x=0.3, this material is Pauli paramagnetic, for x=0.5 it is a charge ordered insulator, for x~0.65–0.75 a Curie Weiss metal, and for x > 0.75 a spin density wave state was suggested [18]. Hydrated sodium cobaltite, $Na_{0.35}CoO_2{\cdot}1.3H_2O$, is a superconductor below approximately 5 K [19,20]. Neutron scattering experiments on $Na_{0.75}CoO_2$ and $Na_{0.82}CoO_2$ showed that magnetic ordering of these structures belongs to the A type of antiferromagnets, with two types of magnetic interactions: ferromagnetic, within a $CoO_2$ layer and antiferromagnetic, between two $CoO_2$ layers [21,22]. Long range antiferromagnetic ordering below 20 K was noticed for 0.75≤x≤0.9 [22].

In our previous work, we studied changes in the structural, microstructural and thermoelectric properties caused by Cu doping [23]. Taking into account all changes of these properties, the aim of this work was to examine the influence of small concentrations of the dopant on magnetic properties (magnetic susceptibility, Curie–Weiss constant and effective magnetic moment) and heat capacity of polycrystalline samples of $NaCo_{2-x}Cu_xO_4$ (x=0, 0.01, 0.03, 0.05) synthesized in two ways, by a mechanochemically assisted solid-state reaction and by the citric acid complex method.

## 2. Materials and methods

Polycrystalline samples of $NaCo_{2-x}Cu_xO_4$ (x=0, 0.01, 0.03, 0.05) were synthesized by a mechanochemically assisted solid-state reaction (MASSR) and a citric acid complex (CAC) method. The detailed procedure was described in our previous work [23]. The MASSR samples were denoted as NCO-MASSR, NCO1-MASSR, NCO3-MASSR, NCO5-MASSR and the CAC samples were denoted as NCO-CAC, NCO1-CAC, NCO3-CAC, and NCO5-CAC.

Sample magnetization was measured using a Quantum Design SQUID MPMS-XL-5 magnetometer in zero field cooled (ZFC) and field cooled (FC) regimes, between 2 K and 300 K and in applied field of 100 Oe. Heat capacity was measured by a Quantum Design Physical Property measurement system (PPMS 9 T), equipped with a 9 T magnet in the temperature range from 2 K to 300 K.

## 3. Results and discussion

The X-ray diffractograms of the MASSR sintered samples contained only peaks of pure γ–$NaCo_2O_4$ (JCPDF card no. 73-0133, space group C2/c) and no additional peaks corresponding to secondary phases were detected [23]. As for the XRD patterns of Cu doped MASSR and CAC samples, only the NCO5-CAC sample showed peaks of the secondary phase (CuO) as reported previously [23].

It is well known that magnetic measurements are highly sensitive to the presence of secondary phases with large magnetic moments. In order to investigate magnetic properties, as well as to verify the phase purity, we measured magnetization of samples in the ZFC and FC regime. Fig. 1 shows the temperature dependence of magnetization of undoped samples in the range between 2 K and 300 K. The NCO-MASSR sample showed a transition at 30 K that was attributed to $Co_3O_4$ (not detected in X-ray diffractograms), confirming the sensitivity of this characterization technique.

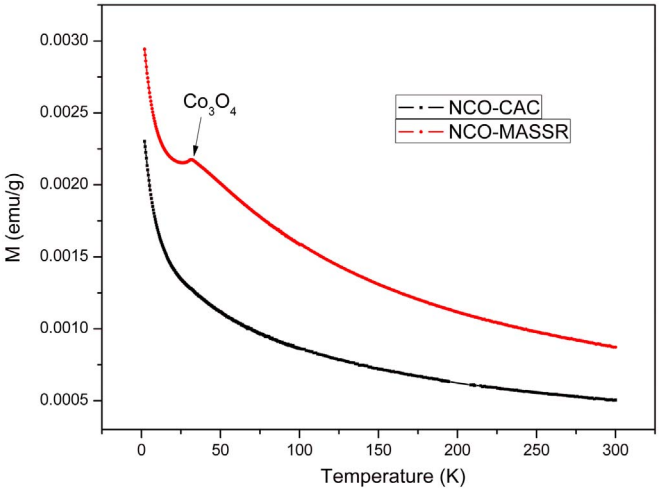


**Fig. 1.** Temperature dependence of the magnetization of undoped MASSR and CAC samples in the temperature range from 2 K to 300 K.

The temperature dependence of the inverse magnetic susceptibility of MASSR and CAC samples measured in the field of 100 Oe between 2 K and 300 K is shown in Fig. 2.

The inverse magnetic susceptibility obeys the Curie-Weiss law (Eq. (1)) in the temperature range between 50 K and 300 K:

$$\chi = \frac{C}{T-\theta}, \tag{1}$$

where $C$ is the Curie and $\theta$ is the Weiss constant. It was noticed that the magnetic susceptibility of MASSR samples decreased with the increase in Cu concentration. This behavior is recognized and reported in literature and can be explained by lowering of the density of states and/or mass enhancement factor [13]. All MASSR samples showed an antiferromagnetic transition at approximately 30 K, which confirmed the presence of a small amount of the $Co_3O_4$ phase [24]. The CAC samples showed this transition only for x≥0.03.

The values of the effective magnetic moments, the Curie and Weiss constants of MASSR and CAC samples are presented in Table 1. All samples showed antiferromagnetic behavior with a negative Weiss constant. The values of $\mu_{eff}$ were calculated based on the Curie constant, which was obtained by linear fitting of the curve $\chi^{-1} = f(T)$ at temperatures above 50 K (Fig. 2). *The $\mu_{eff}$ value* was higher for MASSR samples compared to CAC samples, indicating a larger concentration of low spin $Co^{3+}$ ions (S=0) in CAC samples. In a mean field approximation [25], if only one type of magnetic ions exists, the formula for calculating $\mu_{eff}$ is:

$$\mu_{eff}^2 = xg^2S(S+1)\mu_B^2, \tag{2}$$

where $x$ is the fraction of magnetic ions per formula unit, $g$ is the gyromagnetic factor and $S$ is their spin. Sodium cobaltite contains $Co^{3+}$ and $Co^{4+}$ ions, and we can consider them as two different magnetic systems with the same ordering temperature. Then, the total $\mu_{eff}$ can be expressed as:

$$\mu_{eff}^2 = \mu_{eff1}^2 + \mu_{eff2}^2. \tag{3}$$

To calculate $\mu_{eff}$ of samples without secondary phases, NCO-CAC and NCO1-CAC, we determined the $Co^{4+}$ content in them by inductively coupled plasma optical emission spectroscopy. The content of $Co^{4+}$ ions was 46.5% in NCO-CAC and 48.4% in NCO1-CAC. To be more specific, the molar fraction of $Co^{3+}$ ions is $x_1$=0.535, and $x_2$=0.465 for $Co^{4+}$(with $S_1$=0 and $S_2$=1/2 in the low spin state).

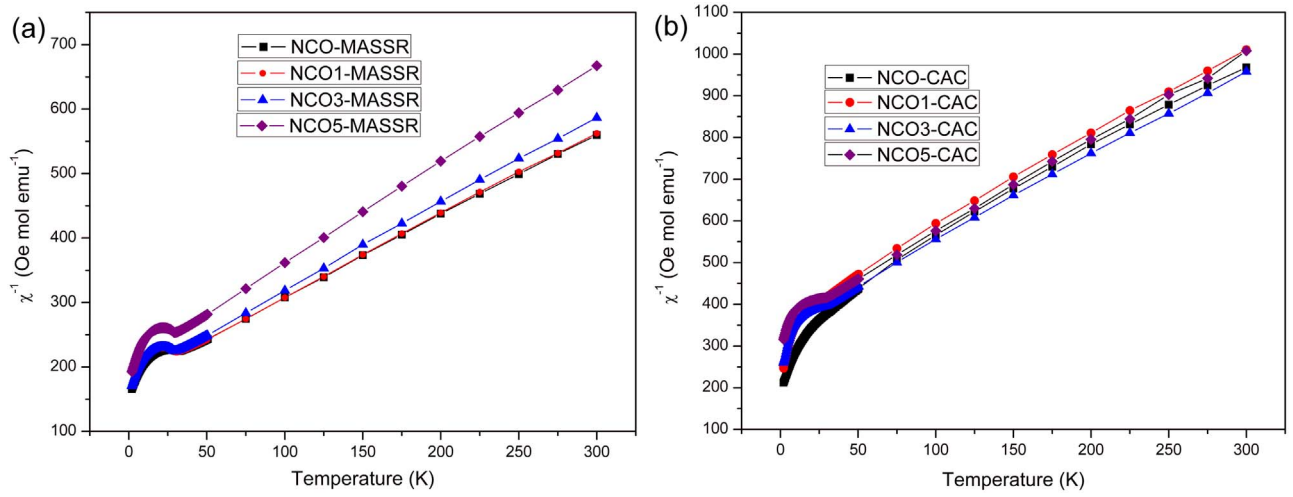


**Fig. 2.** Temperature dependence of the inverse magnetic susceptibility of (a) MASSR and (b) CAC samples measured in the field of 100 Oe.

**Table 1**
Curie constant ($C$), Weiss constant ($\theta$) and effective magnetic moment ($\mu_{eff}$) of MASSR and CAC samples obtained from magnetic measurements.

| mol% Cu | MASSR | | | CAC | | |
|---|---|---|---|---|---|---|
| | $C$ (emu K/ mol Oe) | $\theta$ (K) | $\mu_{eff}$ ($\mu_B$/ atom Co) | $C$ (emu K/ mol Oe) | $\theta$ (K) | $\mu_{eff}$ ($\mu_B$/ atom Co) |
| 0 | 0.3825 | −134.8 | 1.75 | 0.2307 | −161.3 | 1.36 |
| 1 | 0.3783 | −132.7 | 1.74 | 0.2261 | −168.2 | 1.35 |
| 3 | 0.3614 | −130.3 | 1.71 | 0.2430 | −170.7 | 1.40 |
| 5 | 0.3164 | −128.7 | 1.61 | 0.2251 | −158.9 | 1.36 |

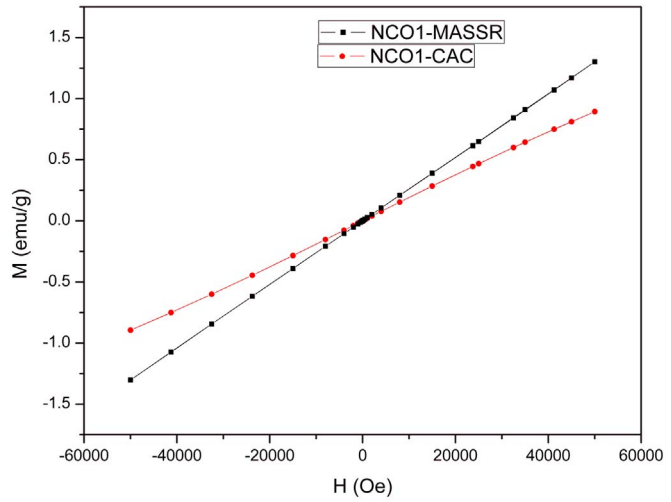


**Fig. 3.** Magnetization as a function of the applied field of NCO1-MASSR and NCO1-CAC samples at 2 K.

Using these results, the last equation leads to $\mu_{eff}$ =1.18$\mu_B$ for the NCO-CAC sample and $\mu_{eff}$ =1.20$\mu_B$ for the NCO1-CAC sample. In both cases, the observed values were lower than the values obtained from the magnetic data (Table 1), implying that the orbital contribution from motions of free electrons must be considered when discussing $\mu_{eff}$. The extent to which the orbital coupling affects the overall $\mu_{eff}$ is determined by the spin-orbit coupling constant ($\lambda$). If we take into account the orbital contribution, the overall $\mu_{eff}$ will be [26]:

$$\mu_{eff} = \mu(spin - only)\left(1 - \frac{\alpha\lambda}{\Delta_{oct}}\right), \quad (4)$$

where $\alpha$ is a constant that depends on the ground term (for an A

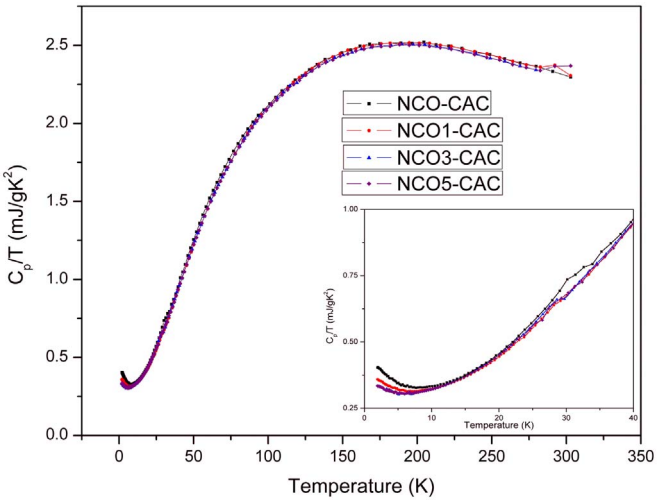


**Fig. 4.** Temperature dependence of the heat capacity of NCO-CAC, NCO1-CAC, NCO3-CAC and NCO5-CAC samples in the temperature region between 2 K and 300 K. The inset shows the Cp/T-T relation in the low temperature range.

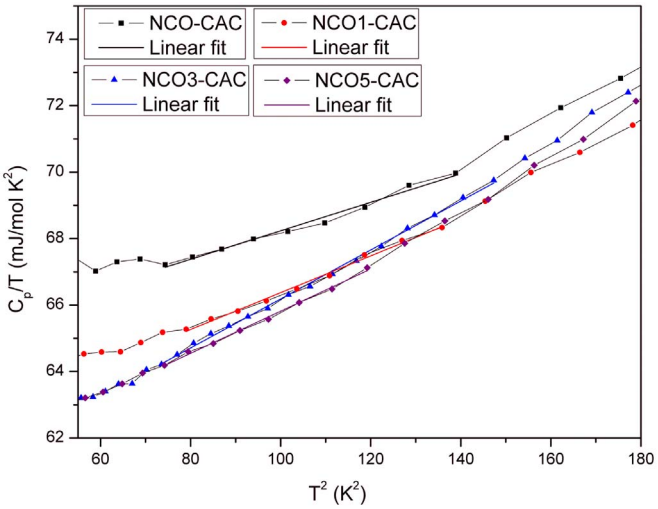


**Fig. 5.** $C_p/T$ as a function of $T^2$ of NCO-CAC, NCO1-CAC, NCO3-CAC and NCO5-CAC samples in the temperature range between 7 K and 13 K; the straight lines are the results of the linear fit in the temperature range between 8 K and 12 K.

**Table 2**
Parameters $\gamma$ and $\beta$ obtained after fitting Eq. (5).

| mol% Cu | $\gamma$ (mJ/mol K$^2$) | $\beta$ (mJ/mol K$^4$) |
|---|---|---|
| 0 | 63.9 ± 0.2 | 0.043 ± 0.002 |
| 1 | 60.8 ± 0.2 | 0.055 ± 0.002 |
| 3 | 58.8 ± 0.1 | 0.074 ± 0.001 |
| 5 | 59.5 ± 0.2 | 0.063 ± 0.002 |

ground state, $\alpha$=4, and for an E ground state, $\alpha$=2), $\Delta_{oct}$ is the crystal field splitting parameter. $\lambda$ is negligible for light atoms, but increases with increase of atomic weight, and for heavier elements the orbital contribution is significant (for the second and the third row of d-elements $\lambda$ is an order of magnitude larger than for the first row). Also, this constant is negative for ions with more than half-filled shells, accordingly for Co ions, too [27]. Therefore, the positive term $>1$ in the parentheses yielded higher $\mu_{eff}$ obtained from magnetic measurements (Table 1) than calculated from optical emission measurements considering the spin only value.

Isothermal magnetization at 2 K as a function of the applied magnetic field M (H) was measured in all samples. All obtained M (H) curves were linear (for NCO1-MASSR and NCO1-CAC they are shown in Fig. 3 similar to those observed in an antiferromagnetic system like NCO [28], confirming the antiferromagnetic ground state of our compounds.

Stabilization of electronic states in systems with strong electron correlation, like NCO, can be greatly affected by the thermodynamic conditions during interactions between spin, charge and orbitals. As a consequence, some properties can be significantly changed in the studied material with small changes in the crystal lattice or in charge concentration [29,30]. Considering that in our case $Cu^{2+}$ replaced $Co^{3+}$ and $Co^{4+}$, we investigated how this change affected $C_p$. Although the samples with no secondary phases (NCO-CAC and NCO1-CAC) were of interest, to gain a broader perspective we measured the heat capacity of all CAC samples in the temperature range between 2 K and 300 K (Fig. 4) and determined the electronic specific heat coefficient. To emphasize the linearity of the electronic heat capacity, we presented the data in the form of $C_p/T=f(T)$.

The total heat capacity, which involves the electronic and phonon part, is given as:

$$C_p/T = \gamma + \beta T^2 + \beta_5 T^4 + \beta_7 T^6, \quad (5)$$

where $\gamma$ is the electronic specific heat coefficient and $\beta$, $\beta_5$, $\beta_7$ are the fitting parameters [31]. In general, the electronic part of the heat capacity dominates at low temperatures and is linear with temperature [32]. To demonstrate that our results were well-described by the simplified Debye formula, high order terms $\beta_5$ and $\beta_7$ in the previous equation were neglected. Thus, by fitting the graph $C_p/T=f(T^2)$ in the low temperature region (7–13 K) we obtained a straight line, and the $\gamma$ value as the interception on the $y$-axis (Fig. 5). The values of $\gamma$ and $\beta$ were presented in Table 2.

As $C_p/T$ at 2 K (inset in Fig. 4) decreased with the increase in Cu content, this indicated that the decrease of the electronic specific heat coefficient came as a result of increase in charge concentration [13]. Since $\gamma$ is proportional to the density of states and mass enhancement factor, the results suggested that lowering of at least one of them would occur with the addition of Cu. The value of $C_p/T$ at 10 K is approximately 70 mJ/molK$^2$, while by fitting the curve $C_p/T=f(T^2)$ we obtained around 60 mJ/molK$^2$ for $\gamma$ at the same temperature, which was comparable with 54 mJ/molK$^2$ reported elsewhere [31]. Sodium cobaltite has a metallic character originating from its high carrier density ($n$=$10^{21}$–$10^{22}$ cm$^{-3}$) in $CoO_2$ layers. Comparing $\gamma$ of our samples with $\gamma$ of some metals, we noticed that our values were significantly higher ($C_p/T$ for copper at 10 K is 6 mJ/molK$^2$) [31]. The high values of the electronic specific heat coefficient are an indicator for strong electron correlation in this type of compounds [33].

The average valence value of the Co ion in stoichiometric NCO is 3.5+ [13]. The highest occupied orbital is $a_{1g}$ and the largest part of the Fermi surface makes a narrow $a_{1g}$ bond. However, after hybridization between the $a_{1g}$ and $e'_g$ orbitals, a broad $a_{1g}$+$e'_g$ bond forms, touches the Fermi level and makes another Fermi surface. Thus, both Fermi surfaces are responsible for the dependence of $\chi$ and $\gamma$ on the amount of Cu. Terasaki et al. [13] assumed that Cu doping affected only the $a_{1g}$ orbital and revealed that Cu substitution enhances the Peltier conductivity from 4 to 100 K, indicating that the mobility is enhanced by Cu. As a consequence of an increase in charge carrier concentration caused by addition of Cu, the mass enhancement was repressed (the mobility of carriers increased), interactions between $a_{1g}$ and $e'_g$ orbitals increased, and as a final result $\chi$ and $\gamma$ decreased [13].

## 4. Conclusions

Polycrystalline samples of $NaCo_{2-x}Cu_xO_4$ (x=0, 0.01, 0.03 and 0.05) were synthesized using two methods: a mechanochemically assisted solid-state reaction and a citric acid complex method. The magnetic susceptibility data showed that the $Co_3O_4$ secondary phase was detected in all MASSR and the CAC samples for x≥0.03. The Weiss constant was negative for all samples, confirming an antiferromagnetic behavior. The effective magnetic moment was lower for CAC samples compared to MASSR samples, indicating the presence of low spin $Co^{3+}$ in the CAC samples. As the fraction of $Co^{3+}$ and $Co^{4+}$ ions in the single phase CAC samples could be determined, the calculated $\mu_{eff}$ was higher than the values obtained from experimental curves. This demonstrated that the orbital contribution must be considered when evaluating the effective magnetic moment. The increase in Cu concentration also caused a decrease of the electronic specific heat coefficient. In general, both the magnetic susceptibility and the electronic specific heat coefficient decreased with the increase in Cu content, pointing at the reduction of the mass enhancement due to the stronger interaction between $a_{1g}$ and $e'_g$+$a_{1g}$ orbitals.

## Acknowledgements

This work was supported by the Serbian Ministry of Education, Science and Technological Development through Project no. III45007.

## References

[1] I. Terasaki, Y. Sasago, K. Uchinokura, Large Thermopower in a Layered Oxide $NaCo_2O_4$, 1999. ⟨http://arxiv.org/abs/cond-mat/9903162v1⟩ (accessed 01.09.16).
[2] J.J. Ding, Y.N. Zhou, Q. Sun, X.Q. Yu, X.Q. Yang, Z.W. Fu, Electrochemical properties of P2-phase $Na_{0.74}CoO_2$ compounds as cathode material for rechargeable sodium-ion batteries, Electrochim. Acta 87 (2013) 388–393.
[3] J. Molenda, D. Baster, M. Molenda, K. Świerczeka, J. Tobolac, Anomaly in the electronic structure of the $Na_xCoO_{2-y}$ cathode as a source of its step-like discharge curve, Phys. Chem. Chem. Phys. 16 (2014) 14845–14857.
[4] P. Kumar, P. Srivastava, J. Singh, R. Belwal, M. Kumar Pandey, K.S. Hui, K.N. Hui, K. Singh, Morphological evolution and structural characterization of bismuth telluride ($Bi_2Te_3$) nanostructures, J. Phys. D: Appl. Phys. 46 (2013) 285301–285309.
[5] I. Terasaki, Y. Sasago, K. Uchinokura, Large thermoelectric power in $NaCo_2O_4$ single crystals, Phys. Rev. B 56 (1997) R12685–R12687.
[6] S. Bhattacharya, S. Rayaprol, A. Singh, A. Dogra, C. Thinaharan, D.K. Aswal, S.K. Gupta, J.V. Yakhmi, R.N. Kulkarni, S.M. Yusuf, S.N. Bhatia, Low temperature thermopower and electrical transport in misfit $Ca_3Co_4O_9$ with elongated $c$-axis, J. Phys. D: Appl. Phys. 41 (2008) (085414–1–085414–5).
[7] M. Von Jansen, R. Hoppe, Notiz zur kenntnis der oxocobaltate des natriums, Z. Anorg. Allg. Chem 408 (1974), 1974, pp. 104–106.
[8] C.M. Bhandari, D.M. Rowe, CRC Handbook of Thermoelectrics, CRC Press, Boca Raton, 1995.
[9] Q. Huang, B. Khaykovich, F.C. Chou, J.H. Cho, J.W. Lynn, Y.S. Lee, Structural transition in $Na_xCoO_2$ with x near 0.75 due to Na rearrangement, Phys. Rev. B 70 (2004) 134115–134116.
[10] J.W. Fergus, Oxide materials for high temperature thermoelectric energy conversion, J. Eur. Ceram. Soc. 32 (2012) 525–540.
[11] W. Koshibae, K. Tsutsui, S. Maekawa, Thermopower in cobalt oxides, Phys. Rev. B 62 (2000) 6869–6872.

[12] J. Sugiyama, H. Itahara, J.H. Brewer, E.J. Ansaldo, T. Motohashi, M. Karppinen, H. Yamauchi, Static magnetic order in $Na_{0.75}CoO_2$ detected by muon spin rotation and relaxation, Phys. Rev. B 67 (2003) 214420–214425.
[13] I. Terasaki, I. Tsukada, Y. Iguchi, Impurity-induced transition and impurity-enhanced thermopower in the thermoelectric oxide $NaCo_{2-x}Cu_xO_4$, Phys. Rev. B 65 (2002) 195106–195107.
[14] S. Hébert, S. Lambert, D. Pelloquin, A. Maignan, Large thermopower in a metallic cobaltite: the layered Tl-Sr-Co-O misfit, Phys. Rev. B 64 (2001) 172101–172104.
[15] S. Wenger, Synthesis and Properties of Thermoelectric Cobalt Oxides (Diploma thesis Empa), Swiss Federal Laboratories for Materials Testing and Research, 2006.
[16] R. Ray, A. Ghoshray, K. Ghoshray, S. Nakamura, $^{59}$Co NMR studies of metallic $NaCo_2O_4$, Phys. Rev. B 59 (1999) 599454–599461.
[17] B. Raveau, Transition metal oxides: promising functional materials, J. Eur. Ceram. Soc. 25 (2005) 1965–1969.
[18] M.L. Foo, Y.Y. Wang, S. Watauchi, Charge ordering, commensurability, and metallicity in the phase diagram of the layered $Na_xCoO_2$, Phys. Rev. Lett. 92 (2004) 247001–247004.
[19] K. Takada, H. Sakurai, E. Takayama-Muromachi, F. Izumi, R.A. Dilanian, T. Sasaki, Superconductivity in twodimensional $CoO_2$ layers, Nature 422 (2003) 53–55.
[20] R.E. Schaak, T. Klimczuk, M.L. Foo, R.J. Cava, Superconductivity phase diagram of $Na_xCoO_2{\cdot}1.3H_2O$, Nature 424 (2003) 527–529.
[21] A.T. Boothroyd, R. Coldea, D.A. Tennant, D. Prabhakaran, L.M. Helme, C.D. Frost, Ferromagnetic in-plane spin fluctuations in $Na_xCoO_2$ observed by neutron inelastic scattering, Phys. Rev. Lett. 92 (2004) 197201–197204.
[22] S.P. Bayrakci, I. Mirebeau, P. Bourges, Y. Sidis, M. Enderle, J. Mesot, D.P. Chen, C.T. Lin, B. Keimer, Magnetic ordering and spin waves in $Na_{0.82}CoO_2$, Phys. Rev. Lett. 94 (2005) (157205–1–157205–4).
[23] S. Pršić, S.M. Savić, Z. Branković, S. Vrtnik, A. Dapčević, G. Branković, Mechanochemically assisted solid-state and citric acid complex syntheses of Cu-doped sodium cobaltite ceramics, J. Alloy. Compd. 640 (2015) 480–487.
[24] I.M. Khriplovich, E.V. Kholopov, I.E. Paukov, Heat capacity and thermodynamic properties of $Co_3O_4$, from 5 to 307 K Low-temperature transition, J. Chem. Thermodyn. 14 (1982) 207–217.
[25] S. De Brion, F. Ciorcas, G. Chouteau, P. Lejay, P. Radaelli, C. Chaillout, Magnetic and electric properties of $La_{1-\delta}MnO_3$, Phys. Rev. B 59 (1999) 1304–1310.
[26] Lecture 19: Magnetic Properties and the Nephelauxetic Effect. ⟨http://www.uniroma2.it/didattica/ChimInorg/deposito/lezione30.pdf⟩ (accessed 01.09.16).
[27] G. Mattney Cole, B.B. Garrett, Atomic and molecular spin-orbit coupling constants for 3d transition metal ions, Inorg. Chem. 9 (1970) 1898–1902.
[28] J. Sugiyama, J.H. Brewer, E.J. Ansaldo, B. Hitti, M. Mikami, Y. Mori, T. Sasaki, Electron correlation in the two-dimensional triangle lattice of $Na_xCoO_2$, Phys. Rev. B 69 (2004) 214423–214427.
[29] T. Motohashi, R. Ueda, E. Naujalis, T. Tojo, I. Terasaki, T. Atake, M. Karppinen, H. Yamauchi, Unconventional magnetic transition and transport behavior in $Na_{0.75}CoO_2$, Phys. Rev. B 67 (2003) (064406–1–064406–5).
[30] Y. Tokura, Y. Tomioka, Colossal magnetoresistive manganites, J. Magn. Magn. Mater. 200 (1999) 1–23.
[31] Y. Ando, N. Miyamoto, K. Segawa, T. Kawata, I. Terasaki, Specific-heat evidence for strong electron correlations in the thermoelectric material $(Na,Ca)Co_2O_4$, Phys. Rev. B 60 (1999) 10580–10583.
[32] Heat Capacities of Solids. ⟨http://vallance.chem.ox.ac.uk/pdfs/EinsteinDebye.pdf⟩ (accessed 01.09.16).
[33] M. Blangero, D. Carlier-Larregaray, M. Pollet, J. Darriet, C. Delmas, High-temperature phase transition in the three-layered sodium cobaltite P´3-$Na_xCoO_2$ (x~0.62), Phys. Rev. B 77 (2008) 184116–184118.